



## A STUDY ON SEISMIC ISOLATION SYSTEM USING HIGH-DAMPING RUBBER BEARINGS FOR RESIDENTIAL BUILDINGS IN TURKEY

N. Murota<sup>(1)</sup>, S. Suzuki<sup>(2)</sup>, T. Mori<sup>(3)</sup>, K. Wakishima<sup>(4)</sup>,  
B. Sadan<sup>(5)</sup>, C. Tuzun<sup>(6)</sup>, M. Erdik<sup>(7)</sup>, S. Akkar<sup>(8)</sup>, H. Sucuoglu<sup>(9)</sup>, F. Sutcu<sup>(10)</sup>

<sup>(1)</sup> Senior Manager, Bridgestone Co., [nobuo.murota@bridgestone.com](mailto:nobuo.murota@bridgestone.com)

<sup>(2)</sup> Senior Engineer, Bridgestone Co., [shigenobu.suzuki@bridgestone.com](mailto:shigenobu.suzuki@bridgestone.com)

<sup>(3)</sup> Chief Researcher, Bridgestone Co., [takahiro.mori1@bridgestone.com](mailto:takahiro.mori1@bridgestone.com)

<sup>(4)</sup> Engineer, Bridgestone Co., [kenji.wakishima@bridgestone.com](mailto:kenji.wakishima@bridgestone.com)

<sup>(5)</sup> Manager, OBS Engineering and Consulting Co., [bahadir@obs.com.tr](mailto:bahadir@obs.com.tr)

<sup>(6)</sup> Manager, OBS Engineering and Consulting Co., [ctuzun@gmail.com](mailto:ctuzun@gmail.com)

<sup>(7)</sup> Professor, Kandilli Observatory and Earthquake Research Institute, Bogazici University, [erdik@boun.edu.tr](mailto:erdik@boun.edu.tr)

<sup>(8)</sup> Professor, Kandilli Observatory and Earthquake Research Institute, Bogazici University, [akkar@boun.edu.tr](mailto:akkar@boun.edu.tr)

<sup>(9)</sup> Professor, Middle East Technical University, [sucuoglu@metu.edu.tr](mailto:sucuoglu@metu.edu.tr)

<sup>(10)</sup> Assistant Professor, Istanbul Technical University, [fatih.sutcu@itu.edu.tr](mailto:fatih.sutcu@itu.edu.tr)

### Abstract

Applicability of seismic isolation for residential buildings in Turkey is studied by analytical and experimental approach. High-damping rubber bearings are selected as components of seismic isolation system which is designed according to the recently updated Turkish Seismic Code issued in 2018. Three model buildings of different story height constructed at assumed site in seismic zone are chosen from database and equivalent lateral force procedure, and time history analyses are carried out. The analyses are also conducted for those with curved surface slider system and lead rubber bearing system in selected cases and the results are compared with those of high-damping rubber bearing. The seismic response of the buildings are evaluated and efficiency of the seismic isolation is confirmed. Subsequently, full-scale test specimens of high-damping rubber bearing are developed and subjected to dynamic loading test under test condition following protocol of prototype test specified in the code. The specific values of test conditions, such as compressive force, shear displacement and frequency, are developed based on the design spectra of several projects in Turkey. The results are comprehensively discussed and the applicability of high-damping rubber bearing for seismic isolation of residential buildings in Turkey is concluded with analytical and experimental approaches.

*Keywords: seismic isolation, high-damping rubber bearing, residential building, time history analysis, prototype test*



## 1. Introduction

Turkey is one of countries which are located in highly active seismic zones in the world. In 1999, Kocaeli earthquake of  $M_w=7.4$  and Duzce earthquake of  $M_w=7.2$  hit urban areas and caused huge damages and losses in economy and human lives [1]. In 2019, Istanbul was hit by earthquake with  $M_w=5.8$ , where some panic and damages occurred in the city which has reminded people of the major Istanbul earthquakes in the far past. Seismic isolation (SI) has established status as an effective anti-seismic measures for structures in these decades [2]. In 2011 Great East Japan earthquake, more than 200 SI building located in the area from Sendai to Tokyo have verified effectiveness of SI systems [3]. In Turkey, SI has gained popularity in 2000's, and it has been applied to structures, such as hospitals, airport terminals, viaducts, and approximately 72 structures have been seismically isolated until 2018. Especially application to the hospitals has been increased as top-down measure by Turkish Ministry of Health. However, there is only a few applications of SI in residential buildings. Fig. 1 shows percentage of SI buildings categorized by purpose of building use and types of SI bearings used in Turkey. When we look back on the building damages by past earthquakes in Turkey, it is naturally expected that SI will be implemented more in the residential buildings in Turkey.

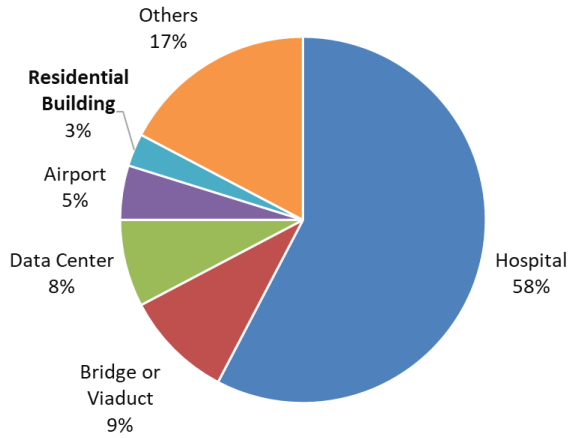
In this study, feasibility of seismic isolation for residential buildings in Turkey is evaluated. Three representative buildings of 5, 10, and 15 stories, which were actually designed as fixed-base systems are selected from database. The buildings are assumed to be constructed in two different sites which are located 10km, and 25 km from one of the active segments of the North Anatolian Fault zone respectively. Target spectra for return period (RP) of 475 years and 2475 years are developed based on the most recent Turkish Seismic Code issued in 2018 (TSC2018) [4, 5]. The SI system using high damping rubber bearing (HDR), which has been recognized as one of most popular seismic isolation devices in Japan, although few application record for structures in Turkey (Fig.1), are designed. Firstly, equivalent lateral force procedure is carried out and the isolator system is designed. Subsequently, nonlinear time history analyses are conducted. A newly developed numerical model for HDR, -Deformation History Integral Type (DHI) model[6, 7]-, is used in this stage. For 10 story buildings, SI systems with curved surface sliders (CSS) and lead rubber bearings (LRB) are also evaluated with time history analyses, and results are compared with the results of HDR system.

In addition to analytical study, dynamic loading test of full scale HDR is carried out following test method specified for prototype tests in TSC2018. Two specimens with diameter of 1000mm are subjected to dynamic loading to investigate the performance whether they adequately satisfy the requirements of the TSC2018. The lamination structure of the test specimen, composed of rubber layers and steel plates, is specially designed to fit the requirements in the code except shear strain limitation of 2.0 at total maximum displacement.

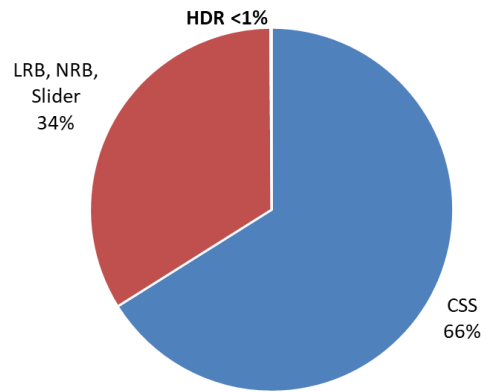
## 2. Numerical analysis

### 2.1 Selection of model buildings

Three buildings were selected as model-structure from many samples in database of Turkish Earthquake Foundation (TDV). All buildings are designed for residential usage and are actual buildings, constructed in the period of 2000 to 2015. Structure type is reinforced concrete (RC), and number of stories are 5, 10, and 15. Table 1 provides geometric characteristics of three buildings. A commercial software ETABS developed by Computers and Structures Inc. was used for analysis works of this study, where the buildings were modelled in 3D. The plan view of the first floor and software model of 10 story building are depicted in Fig.2.



Types of SI structures



\*LRB: Lead Rubber Bearing, NRB: Natural Rubber Bearing

CSS: Curved Surface Slider

Types of isolators

Fig. 1– Types of seismically isolated structures until 2018 (including projects in the planning stage or under construction, surveyed by authors)

Table 1– General properties of selected buildings

Construction period	2000-2015		
Construction material	Reinforced Concrete		
Structural system	Frame or Frame + Shear wall		
Story	5	10	15
Seismic weight	16789 kN	58582 kN	88926 kN

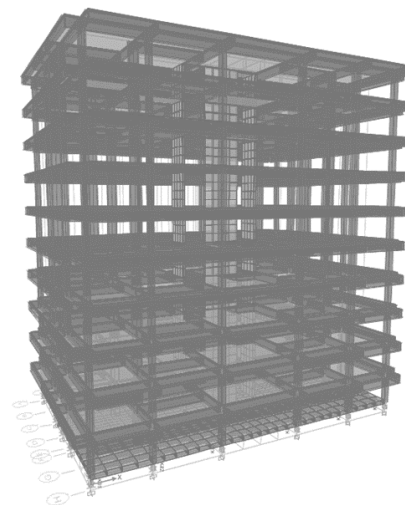
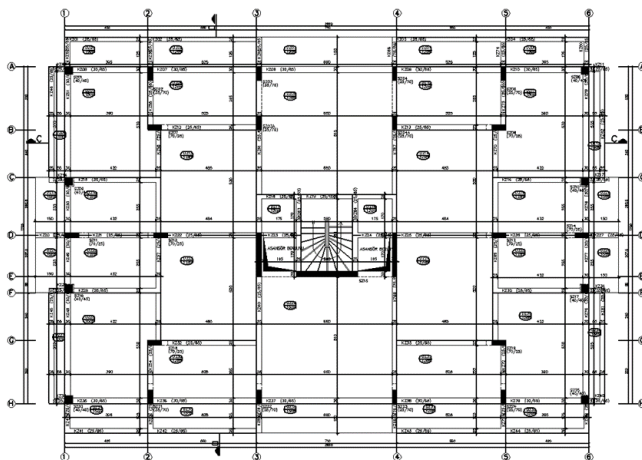


Fig. 2– Plan view and software model of the 10 story model



## 2.2 Design earthquakes

Design earthquakes were developed following TSC2018. The associated design basis short period ( $S_s$ ) and 1s period ( $S_1$ ) spectral acceleration parameters of the design ground motion levels with  $RP=2475$  years (DD-1, or MCE-Maximum Considered Earthquake) and  $RP=475$  years (DD-2, or DBE-Design Basis Earthquake) were obtained directly from the earthquake hazard map of the code. Two specific sites located 10km, and 25km from the most seismically active segments of the North Anatolian Fault zone were considered. Target spectrum established for horizontal direction at each site is shown in Fig.3. The design ground motion records that have been used have following characteristics:

- Magnitudes are between 6.5 and 7.5
- Strike slip type
- Site distance of 25km, site class C (ZC-25):  $360 \text{ m/s} < V_{s30} < 760 \text{ m/s}$
- Site distance of 10km, site class C (ZC-10):  $180 \text{ m/s} < V_{s30} < 650 \text{ m/s}$

where,  $V_{s30}$  is the time-averaged shear-wave velocity to 30 m depth.

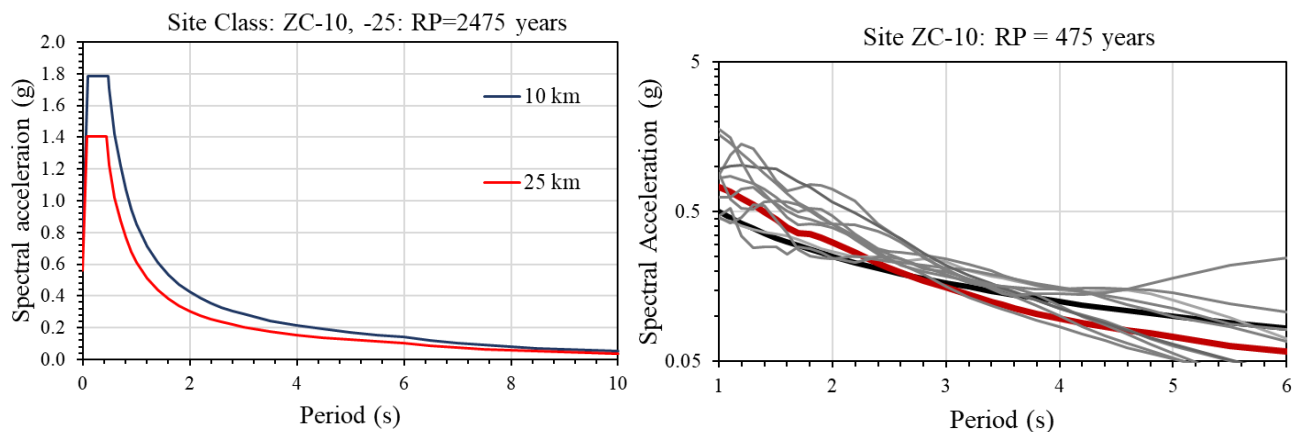


Fig. 3– Target spectra for  $RP=2475$  years and comparison of spectra of eleven records and average of  $RP=475$  years at ZC-10

Total eleven earthquake records for 10, and 25km sites were selected for time history analysis and adequately scaled to fit the target spectra. Scaling was conducted between the range of period of 1 to 6 seconds such that the average of SRSS of scaled records is not less than 90% of the target spectrum according to the code. Fig.3 shows target spectra of  $RP=2475$  years and comparison of target spectrum, scaled eleven records, and average of them, of  $RP=475$  years ground motion. The eleven records applied are listed as follows ( station name in ( ) ):

- For ZC-10km site : 1979 Imperial valley-06(B. Airport), 1979 Imperial valley-06 (EC County C.), 1999 Duzce (362), 1995 Kobe (Port Island), 1995 Kobe (Takatori), 1999 Chi-Chi (CHY074), 2003 Bam (Bam, Iran), 2004 Parkfield-02 CA (EADES), 2004 Parkfield-02 CA (Slack Canyon), 2010-Darfield (DSLCL), 2010 Darfield (GDLC)
- For ZC-25km site : 1979 Imperial valley 06(Sp. Mtn Camera), 1999 Duzce (362), 1999 Hector Mine (Amboy), 1999 Hector Mine (Twentynine Palms), 1999 Chi-Chi (CHY034), 1999 Chi-Chi (CHY042), 1999 Chi-Chi (CHY046), 2000 Tottori (OKYH08), 2000 Tottori (OKYH09), 2010 Darfield (OXZ), 2010 El Mayor Cucupah (Sam W. Stewart)



### 2.3 Design of SI system

Design of seismic isolation system using HDR was conducted following the procedure shown in Fig. 4. As a first step, the HDR seismic isolator for each column was selected based on the long-term load,  $G+0.3Q$  ( $G$ : Dead Load,  $Q$ : Live Load), so as not to exceed nominal load for each size of isolator, which was determined by the manufacturer. Then, equivalent lateral force (ELF) procedure specified in TSC2018 is conducted. The design-target is as follows:

- **Target-1:** Maximum shear strain of isolator including torsional effect under DD-1 with lower bound (LB) characteristics  $\leq$  Allowable maximum shear strain defined by manufacturer
- **Target-2:** Maximum base shear coefficient under DD-2 with upper bound (UB) characteristics  $\leq 0.2$

The allowable maximum shear strain including torsional effect is specified as 200% in TSC2018. However, based on the previous test results by manufacturer, the maximum allowable shear strain applied in this design was expanded to 270%. The stability of the isolator at shear strain of 270% has been verified by various test results. Therefore, allowable maximum shear strain corresponding to the displacement at DD-1 level including torsional effect in this project was decided as 270%. The adequacy of isolation systems was judged by criteria shown as follows. In the judgement by **Criteria-1** and **-2**, the stability of the isolators was evaluated based on the ultimate property diagram (UPD) provided by manufacture. As an example, the UPD of isolator with diameter of 8000mm and total rubber height of 200mm (size code: H80G6-20, later shown in Table2) is shown in Fig. 5. The method for development of UPD has been specified in ISO 22762-2011 Part-3 [8, 9]. The UB and LB characteristics of isolators were determined considering aging (0 at initial and +20% for stiffness and -20% for damping after 60 years), manufacturing tolerance of average of total isolators(+/- 10%), scragging effect (ratio of stiffness and damping for 1<sup>st</sup> cycle to 3<sup>rd</sup> cycle of loading, +15%, 0% respectively). The effect of ambient temperature on the isolator properties were neglected assuming that the isolation system is in conditioned space where expected temperature varies between 0 to 30 Celsius [10]. Additionally, 10 story building was also designed with “lead rubber bearing (LRB)” and “curved surface slider (CSS)” as an alternative SI design in order to compare the performance with the proposed HDR application.

**Criteria-1:** The average seismic response of the buildings, which means average of maximum displacement at DD-1 and maximum base shear at DD-2 in all 11 seismic cases, shall satisfy **Target-1**, and **-2**.

**Criteria-2:** The combination of maximum compressive force and maximum shear displacement shall be within the interaction curve of UPD for each isolator, and maximum shear strain shall be less than 270%.

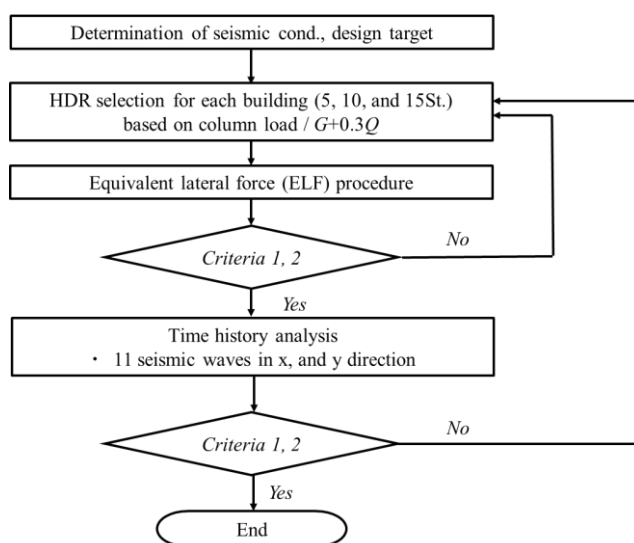


Fig. 4– Design flow of HDR SI system

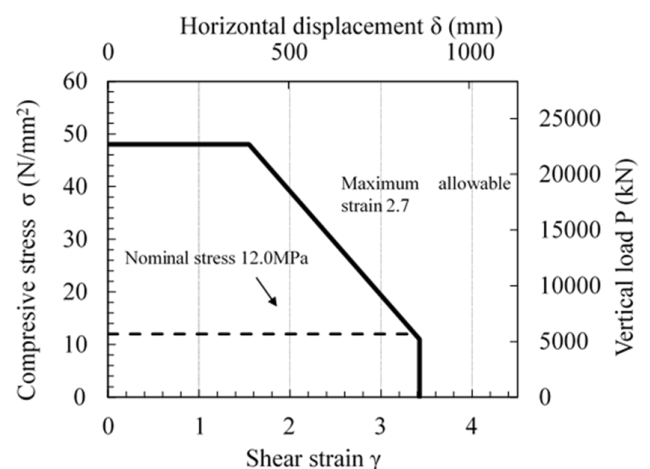


Fig. 5– UPD of 800mm dia. isolator: H80G6-20



The typical characteristics of selected HDRs for each is shown in Table 2. Several different types of HDR isolators were selected. The number in the size code with “H” and two digits indicates the effective rubber diameter in cm unit. There are two different total rubber height, which are 162mm and around 200mm. They are distinguished with symbol of “-16”, and “-20”, and two different compounds, which have shear moduli of 0.39MPa and 0.62MPa at 100% shear strain that are distinguished with symbol of “G4”, and “G6”, respectively. Equivalent damping ratio is 24% at 100% shear strain for both compounds. The nonlinearity of the stiffness and damping ratio were expressed as function of shear strain [11], and the property modification factor  $\lambda$  [4] for each rubber compound, G4 and G6, were determined based on the test results conducted by the isolator manufacturer. The physical properties of both compounds, G4 and G6, are listed in Table 3. The  $\lambda$  are shown in Table 4.

Table 2– Selected isolator size and dimensional characteristics

Building type	Site	Size code	Number of isolators	Typical dimension			Average compressive stress (MPa)
				Effective diameter (mm)	Effective height (mm)	Number of rubber layers	
5 story	ZC-10	H70G4-20	18	700	202	43	2.42
	ZC-25	H60G4-16	18	600	162	41	3.30
10 story	ZC-10	H75G6-20	30	700	202	43	4.69
		H80G6-20	3	750	200	40	
	ZC-25	H60G6-20	5	600	200	50	5.37
		H65G6-20	17	650	198	45	
		H70G6-20	10	700	202	43	
15 Story	ZC-10	H75G6-20	30	750	200	40	5.83
		H80G6-20	4	800	200	37	
	ZC-25	H65G6-20	14	650	198	45	6.65
		H70G6-20	6	700	202	43	
		H75G6-20	10	750	200	40	
		H80G6-20	4	800	200	37	

Table 3– Physical properties of high-damping rubber compound

Rubber compound	Elongation at break (%)	Tensile strength (MPa)	100% modulus (MPa)
G4	min. 840.	min. 7	0.43+/-0.2
G6	min. 780	min. 8.5	0.73+/-0.2

Note: All properties were specified by JIS K 6251 (Japanese Industrial Standards)

Table 4– Property modification factor  $\lambda$  for effective stiffness and equivalent damping ratio

Compound	Condition	$\lambda$ for $K_{eff}$	$\lambda$ for $H_{eq}$
G4	UB	1.52	0.94
	LB	0.90	0.90
G6	UB	1.45	0.94
	LB	0.90	0.90

## 2.4 Equivalent lateral force procedure

Equivalent lateral force (ELF) procedure is an essential analysis defined in all seismic codes in order to determine the basic parameters of the isolation system such as lateral displacement capacity, base shear,



effective period and effective damping ratio. This procedure is useful to perform a preliminary analysis of the isolation system that provides basic response parameters of the system before performing detailed nonlinear response history analysis. The results of ELF for three buildings are shown in Table 5.

Table 5– Summary of ELF results with HDR

Site	ZC-10		ZC-25		
	Building type	Base-shear coeff. at DD-2	Max. iso. disp. at DD-1 (cm)	Base-shear coeff. at DD-2	Max. iso. disp. at DD-1 (cm)
5 story		20.0%	37.8	13.9%	28.0
10 story		16.5%	44.4	12.3%	31.2
15 story		14.1%	51.0	10.6%	36.0

## 2.5 Time history analysis

After completion of ELF procedure, time history analysis was conducted to investigate behavior of the structure and verify adequacy of SI system in detail. The nonlinear response history analyses have been performed using ETABS-CSI software. Numerical model of HDR in ETABS was constructed with nonlinear link element of “High damping rubber bearing” newly implemented since version 17. The basis of the constitutive law is called as deformation history integral type model [12, 13]. The parameter used in the analysis for both HDR compounds is shown in Table 6. Each pair of eleven ground motions was applied simultaneously to the model. Analysis is conducted by Fast Nonlinear Analysis method. Fig.6.shows average value of maximum floor acceleration in 10 story building at ZC-10 under DD-2 ground motion for all cases, and shear force-displacement relationship of one of HDR in x-direction which was set at corner of the building, under DD-1 ground motion of 1995 Kobe (Takatori). The effect of SI is clearly observed at the response acceleration of 1st floor, just above isolation interface, compared with ground acceleration.

Table 6– Modelling parameters for nominal performance of HDR-G6 and HDR-G4

Parameters	HDR - G6 (UB/LB)	HDR - G4 (UB/LB)
$G_a$ (MPa)	0.8136 / 0.5262	0.3220 / 0.1980
$\tau_1$ (MPa)	3.364 / 1.999	1.6430 / 0.932
$\tau_2$ (MPa)	0.4858 / 0.2887	0.457 / 0.259
$\gamma_1$	0.03591	0.03591
$\gamma_2$	0.5	0.3
$\theta$	0.4598	0.5000
$\gamma_d$	0.4181	2.5000

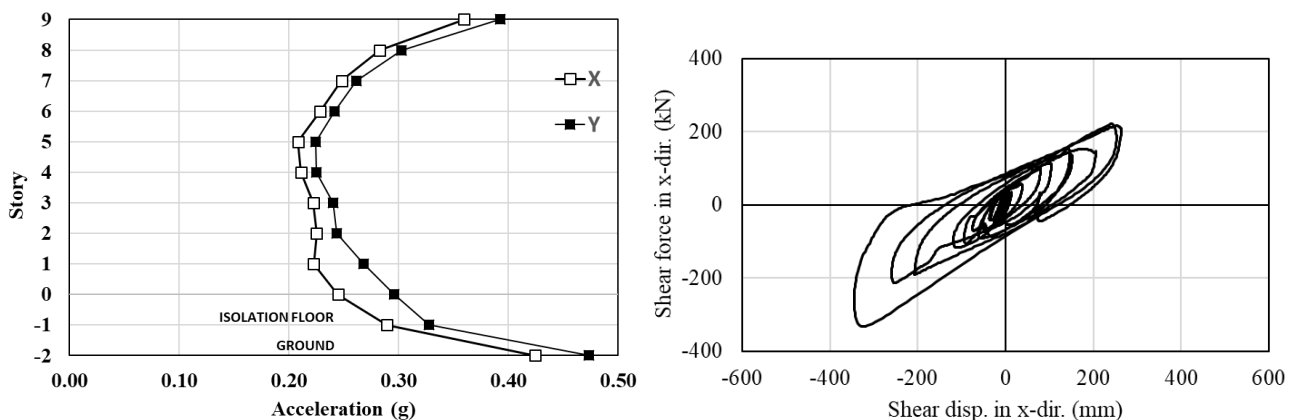


Fig. 6– 10 story building floor response acceleration at ZC-10 under DD-2, and an example of Shear force-disp. relationship of HDR at ZC-10, 1995 Kobe (Takatori) with DHI model under DD-1, x-direction



Average value of base shear coefficient  $V_b/W$  at DD2 with UB characteristics and maximum displacement of isolator  $D_{max}$  with LB characteristics under all earthquakes is summarized in Table 7. In the ZC-10km, the results of base shear in 5 story building exceeded the target value of 20% ( $V_b/W = 21.3\%$ ). The maximum shear strain of HDR was  $0.496/0.20 = 2.485$  in 5 story building at ZC-10 site, which is still less than 2.7 (270%) that is design target of isolator displacement. At the site of ZC-25, all of the results satisfy the design target. The base shear of all three buildings was less than 10%, and shear strain of the isolator was less than 200%. In table 8, the results of 10 story model for varying site and isolator system were compared. In case of LRB, isolators with diameter and number of  $700\text{mm} \times 11\text{pcs.}$ ,  $750\text{mm} \times 17\text{pcs.}$ , and  $800\text{mm} \times 4\text{ pcs.}$  were selected for ZC-10, and  $650\text{mm} \times 20\text{ pcs.}$  and  $700\text{mm} \times 12\text{ pcs.}$  for ZC-25 were selected. Total rubber height of all LRB is 200mm. In case of CSS, isolator with effective radius curve of 5000mm and friction coefficient of 5% for 32 pcs. were selected for both sites. Regarding property modification factor  $\lambda$  for LRB and CSS, default values given in ASCE/SEI 7-16 [10] were used. Although there is some tendency in the results of  $V_b/W$  as  $\text{CSS} < \text{HDR} < \text{LRB}$ , and  $D_{max}$  as  $\text{LRB} < \text{HDR} < \text{CSS}$ , the difference is relatively small and will not make significant impact to the structural behavior. Examples of shear force-shear displacement relationships of LRB and CSS are shown in Fig.7.

Table 7— Results of HDR for all buildings

Story	Result	ZC-10	ZC-25
5 Story	$D_{max}$ (cm)	49.6	25.4
	$V_b/W$	21.3%	9.74%
10 Story	$D_{max}$ (cm)	49.1	26.0
	$V_b/W$	18.3%	8.97%
15 Story	$D_{max}$ (cm)	47.3	29.7
	$V_b/W$	14.2%	8.10%

Table 8— Results in different IS systems

Result	Fault Distance	Isolator Type		
		HDR	LRB	CSS
$V_b/W$	ZC-10	18.3%	20.7%	14.7%
	ZC-25	8.97%	12.1%	11.5%
$D_{max}$ (cm)	ZC-10	49.1	47.9	59.1
	ZC-25	26.0	20.0	27.0

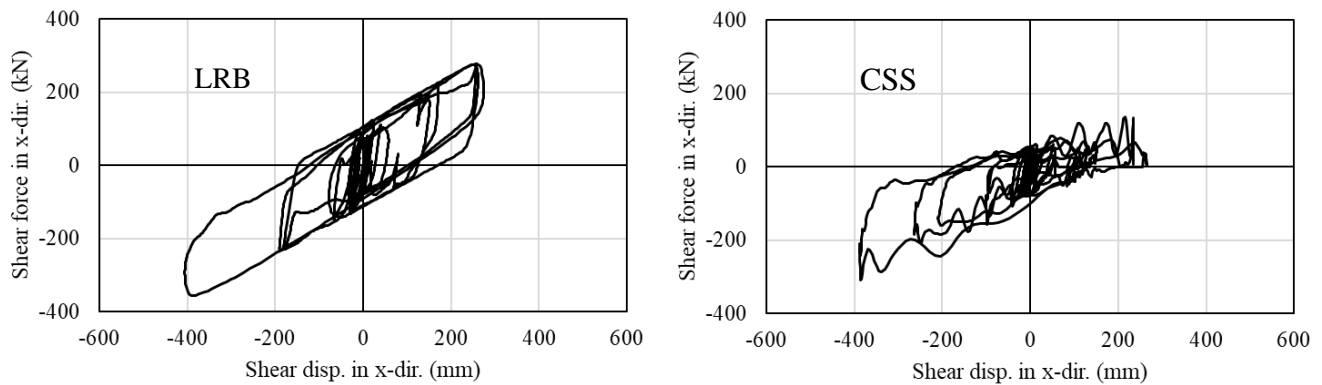


Fig. 7— Examples of shear force-disp. relationships of LRB and CSS at ZC=10km, 1995 Kobe (Takatori), x-direction under DD-1

### 3. Full scale dynamic loading test

In order to demonstrate and verify performance of HDR, full scale dynamic test was conducted in third party testing laboratory. Test conditions and results are summarized as follows. The test specimen has different construction in its lamination of rubber and reinforcing steel plate from original isolators applied in the analysis of this project. Considering application in Turkey based on TSC2018, the maximum compressive stress on isolator is around 7.0 MPa, and a first shape factor  $S_1 (=36)$  as used in original product is not required. Therefore, the test specimen was redesigned and  $S_1$  was around 25.





### 3.1 Test conditions and Specimen

Test was conducted in National Center for Research on Earthquake Engineering (NCREE), Tainan Center, Taiwan.

- (1) Test machine: Bi-Axial Dynamic Testing System (BATS) [11]
- (2) Test specimen: Specimen has a diameter of 1000mm and a total rubber height of 203mm. Shear modulus and equivalent damping ratio of rubber material are 0.62MPa and 24% at 100% shear strain, respectively. Two test specimens, manufactured by Bridgestone Corporation Japan, were used. Basic construction and characteristics are shown in Fig.8 and Table 9.
- (3) Test conditions: Basically, test conditions were determined following TSC2018 Section 14, Table 14.4. Loading conditions such as compressive force and shear displacement were assumed as typical example while referring to several actual projects in Turkey, and was set as follows:

$S_{ae}^{(DD-1)}=0.8g$ , and  $S_{ae}^{(DD-2)}= S_{ae}^{(DD-1)}/1.6=0.5g$ , where  $g$  is gravity acceleration ( $=9.807m/s^2$ ) as indicated in Fig.9. The compressive stress  $\sigma$ , shear strain  $\gamma_D$  at DD-2 and  $\gamma_M$  at DD-1 were determined as follows. Property modification factors  $\lambda$  of isolators were 1.69 at UB and 0.86 at LB for  $K_{eff}$ , and 1.16 at UB and 0.74 at LB for  $h_{eq}$ , respectively. The factors  $\lambda$  applied in this calculation were different from those used in 2.4 and 2.5. Inverse computation of ELF procedure under the given seismic condition were conducted, where maximum shear strain  $\gamma_M$  was assumed as 2.45 ( $=2.7/1.1$ ). The maximum allowable shear strain of the HDR series was 270% which was defined by manufacturer. The results of inverse computation is as follows:  $\sigma=6.0MPa$ ,  $\gamma_D=0.64$ ,  $\gamma_M=2.45$ . In Fig.10, the relationship of response acceleration spectra  $S_a$  at DD-1 and DD-2, and  $F_{iso}/W$  at UB and LB, where  $F_{iso}$  is shear force of isolator and  $W$  is seismic weight of building, and rubber shear strain  $\gamma$  is indicated.

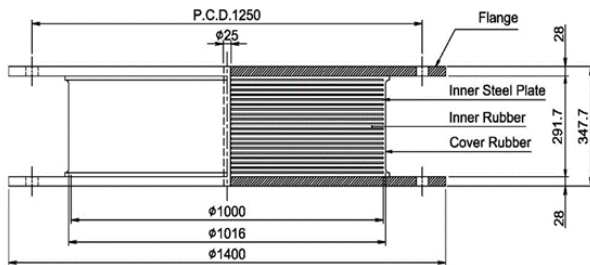


Fig. 8– HDR test specimen

Table 9– Characteristics of test specimen

Outer dia. (Inner dia.)	1000mm (25mm)
Unit rubber thks.	9.7 mm
number of rubber layers	21
Shim plate thickness	4.4mm
First shape factor $S_1$	25.1
Second shape factor $S_2$	4.91
Eff. shear stiff. $K_{eff}$	$2.39 \times 10^3$ (kN/m)
Eq. damp.ratio $h_{eq}$	0.24
Compressive stiffness $K_v$	$5.00 \times 10^6$ (kN/m)
Nominal stress $\sigma_n$	7.2 (MPa)

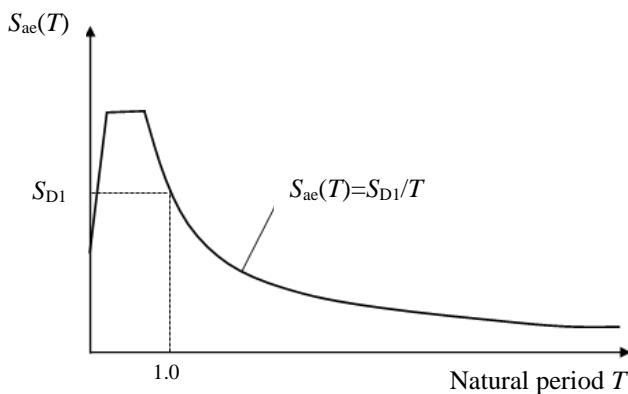


Fig. 9– Response spectra in TSC2018

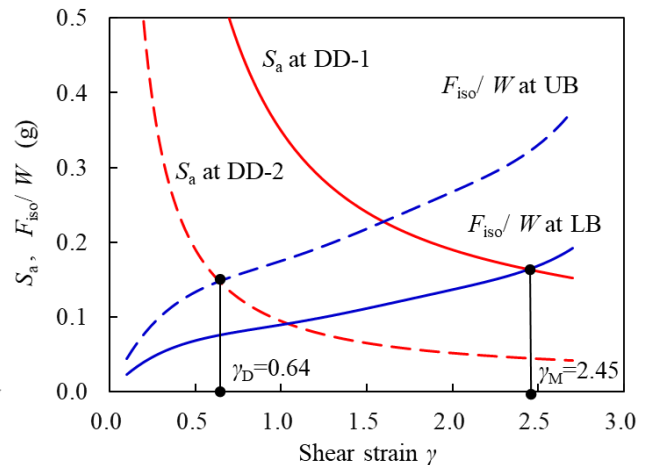


Fig. 10– Relationship of  $S_a$ ,  $F_{iso}/W$ , and  $\gamma$



Loading pattern was decided based on following procedures:

Live load  $Q$  and earthquake load  $E_d$  were assumed in the Eqs. (1) to (3);

$$Q/G=0.3 \quad (1)$$

$$E_d/(G+Q)=1.0 \quad (2)$$

$$W=G+nQ=G+0.3Q \quad (3)$$

where,

$G$  is dead load and  $W$  is seismic weight,

$n=0.3$ , taken for residence.

$W$  is also expressed as,

$$W=A_R \cdot \sigma \quad (4)$$

where,  $A_R$  is effective loaded area of test specimen.

Substituting Eq. (3) to Eqs. (1) and (2), and using Eq. (4) with  $\sigma=6.0\text{MPa}$ , each load pattern specified in TSC2018 is expressed as Table 10. Conditions of displacement is similarly determined and shown in Table 11. Considering small-load control capability of testing machine, 0.217MN and 0.861MN is set as 0.0 MN, and uplift-displacement of 10mm was substituted for -1.73MN.

Table 10– Vertical load conditions

$1.4G+1.6Q$	8.08MN
$G+0.5Q$	4.94MN
$1.2G+0.5Q \pm E_d$	11.4MN / 0.217MN
$1.2G+Q \pm E_d$	12.1MN/ 0.861MN
$0.9G \pm E_d$	9.50MN/-1.73MN

Table 11– Horizontal displacement and isolation period

$D_D=\gamma_D \cdot Hr$	128mm
$D_{TD}=1.1D_D$	141mm
$D_M=\gamma_D \cdot Hr$	490mm
$D_{TM}=1.1D_M$	540mm
$T_D$	1.9 sec
$T_M$	3.5 sec

Test frequency was determined based on isolation period under seismic weight  $W$  and design stiffness under specific displacement. They are set as  $T_D=1.9$  sec and  $T_M=3.5$  sec at  $D_D$  and  $D_M$  respectively.

### 3.2 Test results

As prescribed, test protocol was developed based on TSC2018 and specific value for vertical load and horizontal displacement determined in 3.1. The test results were obtained based on the definitions of characteristics for HDR. Some examples are introduced below.

Prior to start test following protocol of TSC2018, basic performance of the test specimens were evaluated by the test under nominal condition, which is +/-100% shear strain for 3cycles under nominal compressive stress of 7.2MPa and test frequency of 0.33Hz with sinusoidal wave. Table 12 shows shear properties of specimens 1 and 2 obtained by the test under nominal conditions, and Fig.11 shows shear force-displacement relationship of specimen 1. The deviation of the results from nominal value were within 20% for both specimens. Figs. 12 and 13 shows the shear force-displacement relationship of compression and shear test for  $D_D$  and  $D_M$  under vertical load cases of  $G+0.5Q$  and  $1.2G+0.5Q+ E_d$  with test period of  $T_D$  and  $T_M$ , respectively. The plots indicate enough stability in combined large displacement under both vertical load



cases. Even under maximum load case of  $1.2G+0.5Q+E_d$ , curve shows incremental stiffness for all three cycles. Comparing both results, compressive force dependence of shear characteristics are observed. The comparison of effective stiffness and equivalent damping ratio in both cases are shown in Table 13. The results were obtained as taking average of those of all three cycles. Fig. 14 shows the results of ultimate shear capacity tests for  $DT_M$ . Vertical load cases were  $1.2G+Q+E_d$ , 0.0MPa, and -10mm uplift instead of  $0.9G-E_d$ . Even under uplift displacement, no rubber or bonding failure has occurred, and showed proper stability. All of the test results verified the adequate design of HDR test specimen.

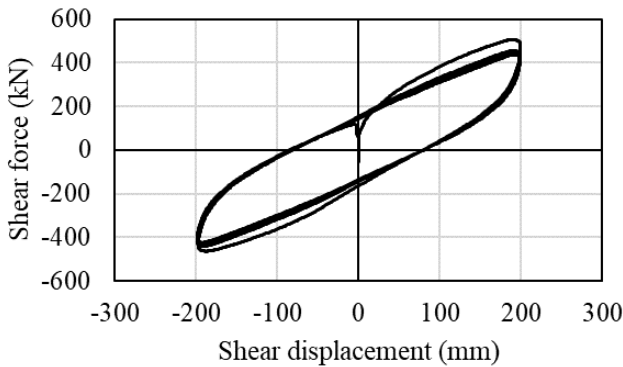


Table 12– Test results under nominal condition

Specimen #	$K_{eff}$ (kN/mm)	$H_{eq}$ (%)
1	2.08 (-13.0%)	20.50 (-14.5%)
2	2.03 (-15.1%)	21.21 (-11.6%)

Fig. 11– Shear force-disp. relationship under nominal condition: Specimen 1,  $\sigma=7.2\text{MPa}$ ,  $\gamma=100\%$

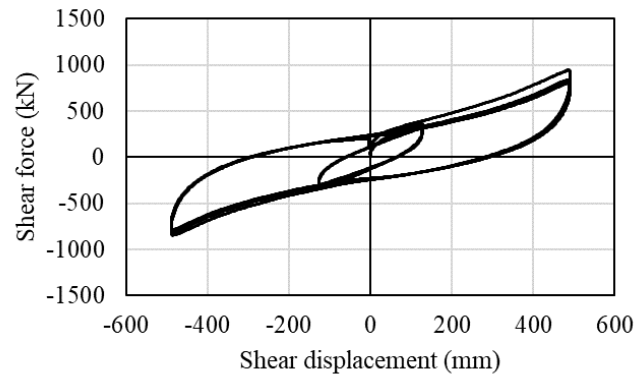
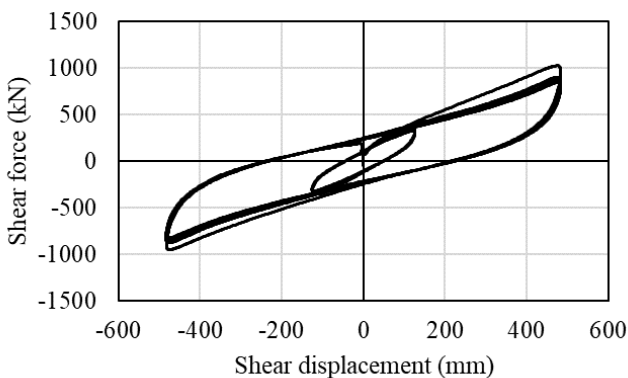


Fig. 12– Shear force-disp. relationship under  $G+0.5Q$

Fig. 13– Shear force-disp. relationship under  $1.2G+0.5Q+E_d$

Table 13– Test results under  $G+0.5Q$  and  $1.2G+0.5Q+E_d$

Comp.load	Shear disp.	$K_{eff}$ (kN/mm)	$H_{eq}$ (%)
$G+0.5Q$	DD-2	2.44	19.55
	DD-1	1.72	18.13
$1.2G+0.5Q+E_d$	DD-2	2.12	24.58
	DD-1	1.52	19.92

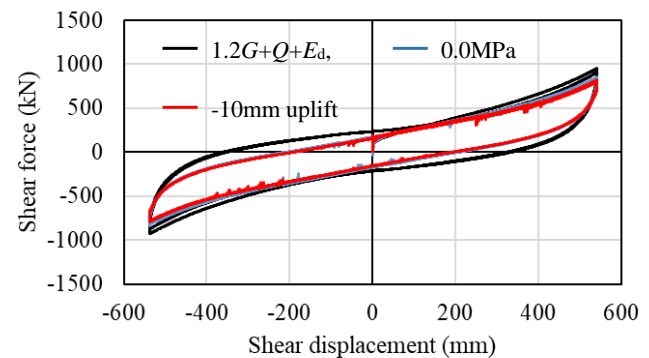


Fig. 14– Shear force-disp. relationship of ultimate property tests



#### 4. Conclusions

Feasibility study on application of SI to residential buildings in Turkey with HDR was conducted by analytical and experimental approaches. Three building models with different height were selected, and SI systems were designed with HDR. Two different sites were supposed and eleven ground motion records were selected for each site. They were scaled to fit the design response spectrum. ELF procedure and time history analyses were carried out. The results clearly demonstrated the effectiveness of SI. A comparison has been made between HDR and other type of SI devices, as well. The differences in the response of structures by SI devices were not significant. Full scale HDR was designed and dynamically tested according to test protocol specified in TSC2018. Test results indicated adequacy of isolator design and sufficient performance. As a general conclusion of this study, the applicability of SI system with HDR system for residential buildings in Turkey was verified.

#### 5. Acknowledgements

Authors would like to express great appreciation to members in National Center for Research on Earthquake Engineering (NCREE) in Taiwan, for their valuable support on dynamic loading test in Tainan center.

#### 6. References

- [1] Erdik M (2001): Report on 1999 Kocaeli and Duzce (Turkey) earthquakes. *Structural Control for Civil and Infrastructure Engineering*, 149-186.
- [2] Murota N (2009): Earthquake Protection Materials - Reviews and Future Directions of Elastomeric Isolators. *Polymers*, Vol.58, No.6, The Society of Polymer Science, Japan (in Japanese).
- [3] Nishi T, Murota N (2012): Elastomeric Seismic-Protection Isolators at the East Japan Giant Earthquake. *10<sup>th</sup> Fall Rubber Colloquium*, Hanover, Germany, KHK.
- [4] *Türkiye Bina Deprem Yönetmeliği 2018*. AFAD, Republic of Turkey (Turkish Building Seismic Code 2018).
- [5] Erdik M, Ulker O, Sadan B, Tuzun C (2018): Seismic Isolation Code Developments and Significant Applications in Turkey. *Soil Dynamics and Earthquake Engineering*, Vol. 115, 413-437.
- [6] Kato H, Mori T, Murota, N, Kikuchi M (2015): Analytical Model for Elastoplastic and Creep-Like Behavior of High-Damping Rubber Bearings. *Journal of Structural Engineering*, ASCE, Vol. 141, Issue 9.
- [7] Masaki M, Mori T, Murota N, Kasai K (2017): Validation of Hysteresis Model of Deformation-History Integral Type for High Damping Rubber Bearings. *Proceedings of 16<sup>th</sup> World Conference on Earthquake Engineering*, Santiago, Chile.
- [8] *ISO 22762-3:2018 Elastomeric seismic-protection isolators - Part 3: Applications for Buildings-Specifications, Annex B*. International Standard Organization.
- [9] Murota N, Kelly JM, Fuller K, Zhou FL, Nishi T, Yoshizawa T, Sudou C, Yazaki F (2006): New International Standard for Elastomeric Seismic-Protection Isolators. *5<sup>th</sup> National Seismic Conference on Bridges & Highways*, San Francisco.
- [10] *ASCE/SEI 7-16 Minimum Design Loads and Associated Criteria for Buildings and Other Structures - Commentary* - , C17.2.8.4, page 679-681, American Society of Civil Engineers.
- [11] Lin WC, Liu CL, Yang CY, Yu CH, Wang SJ, Hwang JS (2019): Seismic Performance Identification of Bi-Axial Dynamic Testing System, *International Conference in Commemoration on 20<sup>th</sup> Anniversary of the 1999 Chi-Chi Earthquake*, Taipei, Taiwan, Sep.15-19, 2019.